Supporting Information

Comparative study of the co-assembly behaviour of 3 chloro-4 hydroxy-phenylazo dyes with DTAB

Wenke Müller,*[a] Ralf Schweins[a], Bernd Nöcker[b], Joachim Kohlbrecher[c], Glen J Smales[d] and Klaus Huber[e]

a. *Institut Laue-Langevin, DS/LSS, 71 Avenue des Martyrs, 38000 Grenoble, France.*

b. *KAO Germany GmbH, Pfungstädter Straße 98-100, 64297 Darmstadt, Germany.*

c. *Paul Scherrer Institut, Forschungsstrasse 111, 5232 Villigen PSI, Switzerland*

d. *Bundesanstalt für Materialforschung und –prüfung, Unter den Eichen 87, 12205 Berlin, Germany*

e. *Universität Paderborn, Warburger Straße 100, 33098 Paderborn, Germany.*

E-mail: we-mue@gmx.net

Experimental

Chemicals. Tetradecyltrimethylammoniumbromide (≥ 99 %) and Cetyltrimethylammoniumbromide (BioXtra, ≥ 99 %) were obtained from Sigma Aldrich and used as received without further purification.

Phase diagrams. Phase diagrams were established by stepwise addition of a Blue stock solution to a surfactant solution. $NaHCO_3/Na_2CO_3$ buffer solution ($\mathrm{pH} = 10.5$, ionic strength $I \approx 0.25\ \mathrm{M}$) was used as a solvent in all cases. The stock solution contained Blue at a molar concentration of 15 mM. The concentration of the surfactant solution was chosen according to the desired sample composition. After each addition of dye stock solution, the sample was vortexed for approximately $30\ \mathrm{s}$ and its visual appearance observed immediately. Phase diagrams were established at room temperature ($\approx 22\ °\mathrm{C}$). It should be noted that at low surfactant-concentrations (below ≈ 9 mM) some initially stable samples showed precipitation after 1 h - 24 h.

UV/vis spectroscopy. UV/vis spectra of solutions containing dye and DTAB were recorded with a Lambda-19 spectrometer from Perkin Elmer. A Hellma quartz glass cuvette with an optical path length of $0.01\ \mathrm{cm}$ was used. The spectrometer was equipped with a thermostat to guarantee a constant measurement temperature of $25\ °\mathrm{C}$. Samples showing precipitation were filtered prior to measurement (MACHEREY-NAGEL, CHROMAFIL Xtra H-PTFE syringe filters, pore size $0.2\ \mathrm{\mu m}$).

Wide-angle X-ray scattering. Wide-angle X-ray scattering (WAXS) was performed on the powder samples of Blue-surfactant precipitates. Data was collected with the MOUSE SAXS/WAXS instrument located at the Bundesanstalt für Materialforschung und –prüfung (BAM, Germany).[1] X-rays were generated from a microfocus X-ray tube, followed by multilayer optics to parallelize and monochromatize the X-ray beams (Cu Kα, λ = 0.154 Å). The scattered radiation was detected using an *in-vacuum* Eiger 1M detector (Dectris, Switzerland), which was placed at multiple distances between 55–2307 mm from the sample. The resulting data has been processed to an absolute intensity scale using the DAWN software package in a standardized complete 2D correction pipeline with uncertainty propagation.[2,3]

Powder samples were prepared by isolation of Blue-surfactant complexes from a phase-separated sample. For this purpose, a stock solution of Blue was added to a stock solution of surfactant to obtain a sample with $[\mathrm{Blue}]_{\mathrm{tot}} = 10\ \mathrm{mM}$ and $[\mathrm{S}]_{\mathrm{tot}} = 20\ \mathrm{mM}$. An aqueous $NaHCO_3/Na_2CO_3$ buffer ($\mathrm{pH} = 10.5$, ionic strength $I \approx 0.25\ \mathrm{M}$) was used as the solvent in all cases. The resulting sample showed phase separation and precipitation of solid dye-surfactant complexes. The samples were equilibrated for $24\ \mathrm{h}$ at room temperature while gently mixing on a roller mixer. Afterwards, the sample was centrifuged and the liquid supernatant decanted. The solid residue was subsequently suspended in MilliQ-water, centrifuged and the liquid decanted again. This washing procedure was repeated two times to remove the buffer salts. The solid remainder was then dried in vacuo at room temperature.

Density. Density measurements were performed using an Anton-Paar Density Meter (DMA 4500 M) requiring a sample volume of 1 mL. Density measurements were performed to be able to calculate apparent molar volumes $V_{\mathrm{m}}(c)$ of solutions of Blue and Red. For this purpose, five solutions containing Blue concentrations between 1 mM (0.37 g L^{-1}) and 20 mM (7.39 g L^{-1}) and eight solutions containing Red concentrations between 0.5 mM (0.14 g L^{-1}) and 10 mM (2.87 g L^{-1}) were prepared in an $NaHCO_3/Na_2CO_3$ buffer (pD = 10.7, I ≈ 0.25) in 100 % D_2O. The densities of these solutions as well as of the buffer were measured after equilibrating the temperature of each sample to 25 °C. This yielded sample densities (ρ) as well as the density of the solvent (ρ_0).

Influence of DTAB addition on dye absorption

Figure SI1 shows the change in position of the absorption maximum of all three dyes upon addition of various concentrations of DTAB.

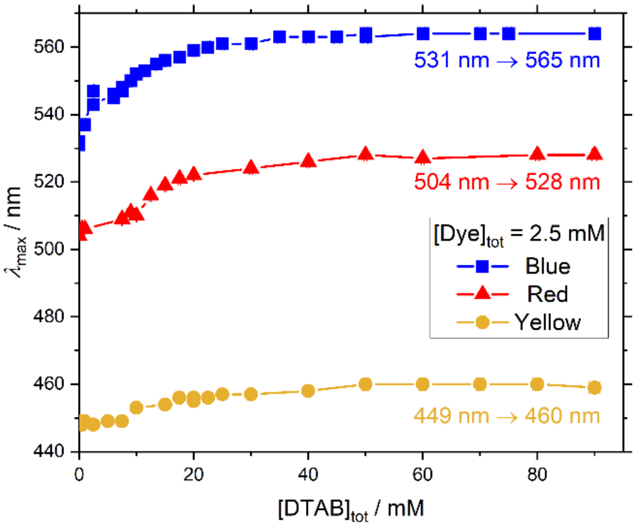

Figure SI1: Extend of change in the position of the dye absorption maximum upon addition of DTAB in $NaHCO_3/Na_2CO_3$ buffer at 25 °C.

Solid dye-surfactant complexes between Blue and cationic surfactants with different chain lengths

Phase diagrams

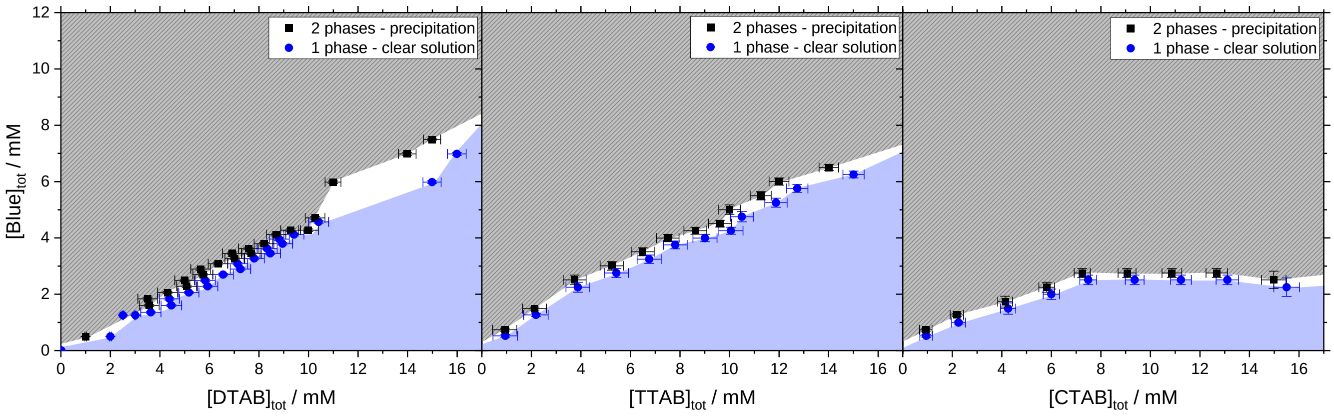

Figure SI2: Concentration-dependent phase behaviour of solutions of Blue in combination with cationic trimethylammoniumbromide surfactants. From left to right with increasing alkyl chain length C_n: Dodecyltrimethylammoniumbromide (DTAB, C_{12}), Tetradecyltrimethylammoniumbromide (TTAB, C_{14}), Cetyltrimethylammoniumbromide (CTAB, C_{16}). An aqueous $NaHCO_3/Na_2CO_3$ buffer (pH = 10.5, $I \approx 0.25$ M) was used as a solvent at all times. Phase diagrams were established at room temperature (≈ 22 °C).

Wide-angle X-ray scattering. Precipitates formed between the dye Blue and the cationic surfactant DTAB in the 2-phase region of the phase diagram were isolated and analyzed by X-ray scattering on the powder sample. The corresponding powder WAXS-curve is shown in Figure SI3 as a black line and displays clearly discernible diffraction peaks.

This points towards crystalline ordering within the Blue-DTAB precipitates. To facilitate the assignment of peaks to structural features of the crystalline precipitates, WAXS curves were also recorded for complexes formed between the dye Blue and the surfactants tetradecyltrimethylammoniumbromide (TTAB) and cetyltrimethylammoniumbromide (CTAB). All three surfactants have the same headgroup and only show a variation in the length of their hydrophobic tail. This variation is reflected in the WAXS-pattern of solid dye-surfactant complexes. The position of the second diffraction peak is shifted from $q = 0.282\ \text{Å}^{-1}$ (DTAB) to $q = 0.244\ \text{Å}^{-1}$ (CTAB) with increasing chain length. Due to the reciprocal relation between the value of q and real-space length scales this is consistent with the length of the hydrophobic tail. Apart from this trend some reflections overlay, suggesting similar structural features independent of surfactant hydrophobic chain length. It was abstained from a more detailed investigation of the structure of Blue-surfactant complexes. A lamellar structure was suggested for similar systems by the Faul group.[4] This is not unlikely for the present system, but needs to be confirmed.

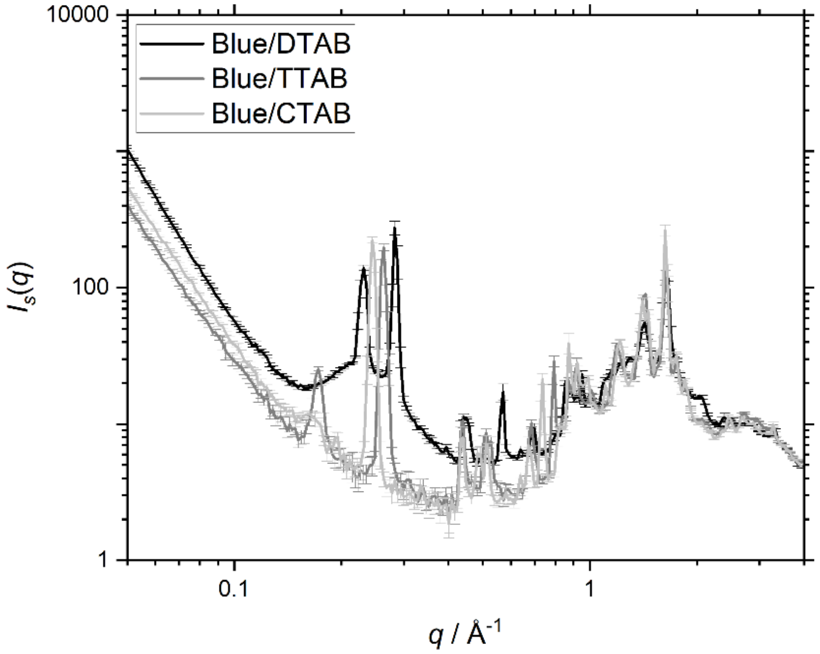

Figure SI3: WAXS-curves of solid complexes between the anionic dye Blue and cationic surfactants with varying hydrophobic alkyl chain lengths C_n: DTAB (C_{12}), TTAB (C_{14}), CTAB (C_{16}).

Analysis of small-angle neutron scattering curves

For the analysis of SANS data, the volume fraction of dye-surfactant assemblies in solution was calculated from the known concentration of dye and surfactant as well as their molar volumes. It was assumed that all dye- and surfactant molecules in the sample take part in assembly formation and that their molar volumes do not change upon interaction. Although both assumptions might not be true due to the existence of a critical micelle concentration, the presence of free molecules up to this concentration and volume compression or expansion effects upon aggregation, it is a useful strategy to reduce the number of parameters that have to be fitted. As the scattering length density (*SLD*) of the overall assembly was fitted and not used for the interpretation of data, the use of slightly incorrect volume fraction should not devalue size parameters obtained from fitting.

Molar volume. Table SI1 summarizes molar volumes used for the calculation of aggregate volume fractions. Molar volumes of Blue and Red were determined by measuring the densities of solutions containing the respective dye at various concentrations c. Details on density measurements can be found in the experimental part. A $NaHCO_3/Na_2CO_3$ buffer (pD = 10.7, $I \approx 0.25$ M) prepared in D_2O was used as a solvent in all cases. Measurements were performed at 25 °C. Apparent molar volumes $V_\mathrm{m}(c)$ were calculated according to the following equation:[5]

$$\mathrm{V_m}(c) = \frac{1000 \cdot (\rho_0 - \rho)}{c \cdot \rho} + \frac{M}{\rho} \tag{1}$$

ρ_0 is the density of the solvent, ρ the density of the solution and M the molar mass of the solute. Extrapolation of $V_\mathrm{m}(c)$ to $c = 0$ yields the molar volume $V_\mathrm{m} = V_\mathrm{m}(c \to 0)$. As in the presented cases of Blue and Red apparent molar volumes $V_\mathrm{m}(c)$ did not depend on sample concentration, their average was calculated to obtain V_m. The molar volume of Yellow was not measured and assumed to correspond to the molar volume of Red.

Table SI1: Molar volumes of several compounds at 25 °C.

Compound	Molar volume V_m / cm^3 mol^{-1}
Yellow*	213.1
Blue	246.3
Red	213.1
DTAB**	302.7

*Assumed to have the same molar volume as Red. **Calculated from molar volumes of methyl-, methylene-, and trimethylammonium groups as well as the molar volume of Br$^-$ employed and reported in literature assuming additivity of molar volumes.[6–8]

SANS fit parameters

Table SI2: Model parameters from form factor fits to SANS curves resulting from solutions containing dye at a concentration of $[\mathrm{Dye}]_{\mathrm{tot}}$ = 5 mM and DTAB at a concentration of $[\mathrm{DTAB}]_{\mathrm{tot}}$ = 30 mM. Samples were prepared in an aqueous $NaHCO_3/Na_2CO_3$ buffer (pD = 10.7, $I \approx 0.25$ M) in D_2O except for the sample containing Blue. For the sample containing Blue the buffer was prepared in a H_2O/D_2O mixture (50:50 v/v) as described in the experimental part in the main document. For fitting the SANS curve emerging from a pure DTAB solution, the product of an oblate ellipsoidal form factor and a structure factor by Hayter and Penfold was used.[9,10] The scattering length density of the solvent was set to a fixed value of $6.376 \cdot 10^{-6}$ Å^{-2} in all cases except for the sample containing Blue, where the solvent was prepared in a H_2O/D_2O mixture (50:50 v/v) and it was set to $2.918 \cdot 10^{-6}$ Å^{-2}. In the case of the form factor model of a triaxial ellipsoid, the length parameter is equivalent to the longest radius.

Dye	Model	Cross Section		Length	*SLD*	ϕ	χ^2
		r_{minor} / Å	r_{major} / Å	*L* / Å	10^{-6} Å^{-2}		
no dye	Oblate ellipsoid x structure factor	r_{eq} = 22.357 ± 0.009		r_{p} = 14.048 ± 0.008	-0.11 ± 0.04	0.00635	12.667
Yellow	Oblate ellipsoid	r_{eq} = 21.73 ± 0.04		r_{p} = 13.98 ± 0.06	1.136 ± 0.006	0.01014	5.5788
Blue	Triaxial ellipsoid	15.3 ± 0.2	22.0 ± 0.3	32.0 ± 0.3	5.778 ± 0.004	0.01031	1.3194
Red	Triaxial ellipsoid	15.93 ± 0.02	22.32 ± 0.03	40.31 ± 0.04	1.239 ± 0.001	0.01015	18.64

r_{p} – polar radius, r_{eq} – equatorial radius, r_{minor} – minor cross section radius, r_{major} – major cross section radius, *L* – length, *SLD* – scattering length density of the scatterer, ϕ – scatterer volume fraction; Parameters for calculating the structure factor in a solution of DTAB without dye: Micellar charge: 15, temperature: 298.15 K, salt concentration = $I \approx 0.25$ M, dielectric constant: 78.06[11]

Table SI3: Model parameters from form factor fits to SANS curves resulting from solutions containing dye at a concentration of $[\mathrm{Dye}]_{\mathrm{tot}}$ = 5 mM and DTAB at a concentration of $[\mathrm{DTAB}]_{\mathrm{tot}}$ = 20 mM. Samples were prepared in an aqueous $NaHCO_3/Na_2CO_3$ buffer (pD = 10.7, $I \approx 0.25$ M) in D_2O. The scattering length density of the solvent was set to a fixed value of $6.376 \cdot 10^{-6}$ Å^{-2} in all cases. In the case of the form factor model of a triaxial ellipsoid, the length parameter is equivalent to the longest radius.

Dye	Model	Cross Section		Length	*SLD*	ϕ	χ^2
		r_{minor} / Å	r_{major} / Å	*L* / Å	10^{-6} Å^{-2}		
Yellow	Triaxial ellipsoid	13.8 ± 0.2	21.6 ± 0.6	24.4 ± 0.6	1.312 ± 0.008	0.00712	1.5499
Blue	Cylinder with elliptical cross section	13.1 ± 0.2	19.6 ± 0.4	*L* = 199 ± 3 σ/L_{avg} = 0.95	1.323 ± 0.006	0.00729	2.0759
Red	Cylinder with elliptical cross section	14.19 ± 0.02	23.64 ± 0.05	*L* = 233.5 ± 0.7 σ/L_{avg} = 0.5	1.493 ± 0.001	0.00713	7.2001

r_{p} – polar radius, r_{eq} – equatorial radius, r_{minor} – minor cross section radius, r_{major} – major cross section radius, *L* – length, σ/L_{avg} - ratio between the root-mean-square deviation from the average length and the average length, *SLD* – scattering length density of the scatterer, ϕ – scatterer volume fraction

References

1 G. J. Smales and B. R. Pauw, *J. Inst.*, 2021, **16**, P06034.

2 J. Filik, A. W. Ashton, P. C. Y. Chang, P. A. Chater, S. J. Day, M. Drakopoulos, M. W. Gerring, M. L. Hart, O. V. Magdysyuk, S. Michalik, A. Smith, C. C. Tang, N. J. Terrill, M. T. Wharmby and H. Wilhelm, *J Appl Cryst*, 2017, **50**, 959–966.

3 B. R. Pauw, A. J. Smith, T. Snow, N. J. Terrill and A. F. Thünemann, *J Appl Cryst*, 2017, **50**, 1800–1811.

4 Y. Guan, M. Antonietti, and Faul, *Langmuir*, 2002, **18**, 5939–5945.

5 C. W. Garland, J. W. Nibler and D. P. Shoemaker, *Experiments in physical chemistry*, McGraw-Hill Higher Education, Boston, 8th ed., 2009.

6 S. S. Berr, *J. Phys. Chem.*, 1987, **91**, 4760–4765.

7 J. B. Hayter and J. Penfold, *Colloid & Polymer Sci*, 1983, **261**, 1022–1030.

8 Y. Marcus, *Ion properties*, Marcel Dekker, New York, 1997.

9 L. A. Feigin and D. I. Svergun, *Structure Analysis by Small-Angle X-Ray and Neutron Scattering*, Springer US, 1987.

10 J. B. Hayter and J. Penfold, *Molecular Physics*, 1981, **42**, 109–118.

11 G. A. Vidulich, D. F. Evans and R. L. Kay, *J. Phys. Chem.*, 1967, **71**, 656–662.